Longitudinal Optical Phonons in Metallic and Semiconducting Carbon Nanotubes

Martin Fouquet,[1] Hagen Telg,[1,*] Janina Maultzsch,[1,2] Yang Wu,[2] Bhupesh Chandra,[3] J. Hone,[3] Tony F. Heinz,[2] and C. Thomsen[1]

[1]*Institut für Festkörperphysik, Technische Universität Berlin, Hardenbergstrasse 36, 10623 Berlin, Germany*
[2]*Departments of Electrical Engineering and Physics, Columbia University, New York 10027, USA*
[3]*Department of Mechanical Engineering, Columbia University, New York 10027, USA*

(Received 26 September 2008; published 19 February 2009)

We analyze the high-energy Raman modes, G^+ and G^-, in a pair of one metallic and one semiconducting nanotubes. By combining Rayleigh scattering with Raman resonance profiles of the radial breathing mode and the high-energy modes, we show that the observed G^- and G^+ peaks can originate from longitudinal optical phonons of different tubes. The G^- peak is the longitudinal mode of the metallic tube; it is broadened and downshifted due to strong electron-phonon coupling in the metallic nanotube. The G^+ peak is due to the longitudinal mode in the semiconducting tube. This result resolves an ongoing debate in the literature.

DOI: 10.1103/PhysRevLett.102.075501 PACS numbers: 63.22.Gh, 61.48.De, 73.22.−f, 78.67.Ch

Raman spectroscopy is a well-established optical method for the characterization of carbon nanotubes [1,2]. While the defect induced D mode offers a tool to estimate the quality of a nanotube sample, the diameter distribution can be obtained from the diameter dependent radial breathing mode (RBM). Because of the unique electronic band structure of carbon nanotubes the exact atomic structure—given by the chiral indices (n_1, n_2)—can be obtained from the RBM in conjunction with the excitation energy [3]. Even without a detailed (n_1, n_2) assignment, the presence of metallic nanotubes in a sample can be detected on the basis of the shape of the high-energy modes (HEM) in the Raman spectrum [4–6]. Between 1540 and 1600 cm^{-1}, the Raman spectrum of a typical carbon nanotube sample—containing a large variety of chiral indices—shows two characteristic HEM features which are commonly referred to as G^- (lower frequency) and G^+ (higher frequency). Compared with the RBM the high-energy modes are less diameter dependent and the resonance windows are up to a magnitude wider. Therefore, the HEM is often formed by overlapping signals of different tubes. While both features appear as reasonably sharp peaks when mainly semiconducting nanotubes are resonantly excited (full width at half maximum: FWHM ~10 cm^{-1}), the G^- peak is broadened and downshifted when mainly metallic nanotubes are in resonance [7]. In the following we use the terms metallic G^- and semiconducting G^-, when referring to a broad and a narrow G^- peak, respectively. In the case of semiconducting nanotubes, G^+ and G^- are attributed to the LO and TO phonon, respectively, where LO refers to the axial (longitudinal optical) and TO to the circumferential (transverse optical) displacement of the atoms [8,9]. For metallic nanotubes, the assignment of the G^- and G^+ Raman peaks to the TO and LO phonons is still under debate with contradicting conclusions appearing in the literature [8–15].

Two different models have been developed for the description of the peculiar line shape of the high-energy Raman modes (G^- and G^+) in metallic carbon nanotubes. The first model [10] proposed phonon-plasmon interactions as the origin of the metallic line shape. According to this model, the linewidth increases with the thickness of the nanotube bundle. The G^- and G^+ features were assigned in Ref. [10] to the TO and LO phonon, respectively, as in semiconducting tubes. More recent models attribute the broadening of the metallic G^- to strong coupling between the LO phonon and electronic excitations [9,11,12]. This coupling causes a dramatic softening of the LO frequency and a broadening of the Raman line. As a result, the frequency of the LO phonon drops below the frequency of the TO phonon in metallic nanotubes [9,11,12]. This theory explains the metallic G^- and, in particular, the large Raman linewidth as an intrinsic property of a single metallic tube and is consistent with recent experiments on free-standing metallic nanotubes and on graphene [13,16]. In this model—due to the strong electron-phonon coupling—the LO frequency is below the TO frequency, and consequently the G^- peak is assigned to the LO phonon. In some Raman measurements on what were presumed to be single metallic nanotubes, the G^+ peak has been reported at 1590 cm^{-1} [17–19]. Consequently this peak would have to be assigned to the TO phonon in metallic tubes. However, the TO phonon in metallic tubes is expected to have a similar frequency to that of the TO mode in semiconducting tubes, which is below 1590 cm^{-1} [9,12]. The question therefore arises how to assign the G^+ peak at 1590 cm^{-1}.

In this Letter we show that the presence of a G^+ peak at ~1590 cm^{-1} in a typical "metallic" Raman spectrum often indicates the presence of an additional semiconducting nanotube. We performed Rayleigh and resonant Raman measurements on a pair of one metallic and one semi-

conducting carbon nanotube forming a small bundle freely suspended in air. By varying the excitation energy we observed a changing line shape for the high-energy G^+ and G^- Raman modes. We see a broad metallic G^- peak at 1540 cm^{-1} and a narrow G^+ peak at 1590 cm^{-1} with maximum Raman intensities at different excitation energies. Including results from Rayleigh scattering experiments and radial breathing mode (RBM) Raman spectra, we can relate the peak at 1540 cm^{-1} to the longitudinal mode of the metallic tube which is broadened due to the strong electron-phonon coupling, while the peak at 1590 cm^{-1} originates from the semiconducting tube.

Rayleigh and resonant Raman scattering experiments were performed on a pair of one metallic and one semiconducting nanotube a side-product of single-nanotube growth. The nanotubes were grown in a chemical vapor-deposition process using CoMo-doped mesoporous silica catalyst particles. To minimize possible interactions with the environment [20] tubes were grown across a 100 μm wide slit with the growth direction defined by the gas flow in the furnace [21]. Raman measurements were performed on a confocal micro-Raman setup (Dilor XY800; objective: $\times$100; NA: 0.8); the spectra were recorded with a charge coupled device. The Raman excitation energy was varied between 1.87 and 2.15 eV using a tunable dye laser. To prevent laser induced heating, we limited the laser power to $\approx$ 200 μW [22,23]. All spectra were normalized to laser power and integration time. In order to correct the Raman intensities for the system response, we normalized each spectrum to the intensity of the Raman signal of CaF_2 (321 cm^{-1}). Rayleigh-scattering measurements were performed using a white-light source and detected in a dark field geometry as described in Ref. [24] The detection range was between 1.24 and 2.76 eV. In both experiments we located the tubes by scanning the laser or white-light focus along the slit until a bright scattering spot was seen, indicating the presence of freely suspended tubes.

In Fig. 1 we plot the Rayleigh spectrum of our nanotube sample. The spectrum shows three peaks at 1.937, 2.055, and 2.206 eV. Considering tube diameters between 1 and 2.5 nm, there is no single nanotube with three transitions predicted in this energy range. Therefore our sample must consist of a small bundle of two or more nanotubes. We will show below that it is indeed a pair of nanotubes, one semiconducting and one metallic.

Figure 2(a) shows the HEM Raman spectra for all excitation energies. The spectra show two peaks, a broad peak (metallic G^-) at 1540 cm^{-1} (FWHM = 48.5 cm^{-1}) and a narrow peak (G^+) at 1590 cm^{-1} (FWHM = 5.6 cm^{-1}). In addition, a small shoulder at 1580 cm^{-1} is seen. In the Raman spectrum excited at 2.04 eV [Fig. 2(b)] both G^- and G^+ are present. Because of the metallic G^- peak this spectrum would typically be assigned to a metallic nanotube [7,17,19,25]. While the broad peak (G^-) has its maximum intensity at 1.94 eV excitation energy, the narrow peak (G^+) appears only at excitation energies above this energy. This implies that the G^- and G^+ peaks originate from different nanotubes with different resonance energies, confirming the conclusion from the Rayleigh experiment that we have at least two tubes. In the following we show that the spectrum in Fig. 2(b) can easily be explained if only the broad peak (G^-) is related to a metallic tube, whereas G^+ originates from a semiconducting tube.

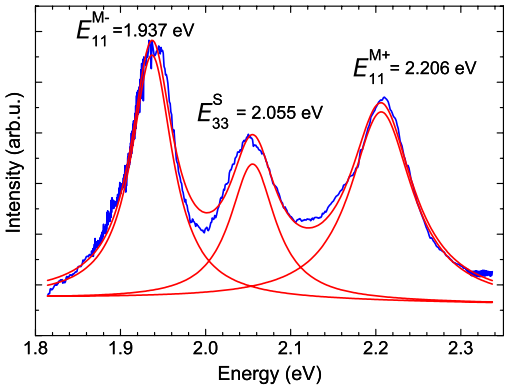

FIG. 1 (color online). Rayleigh-scattering spectrum of a pair of nanotubes. Peaks at 1.937 and 2.206 eV are assigned to the lower E_{11}^{M-} and upper E_{11}^{M+} transition of the first optical transition in the metallic (12,3) tube. The peak at 2.055 eV originates from the third optical transition E_{33}^{S} in a semiconducting tube.

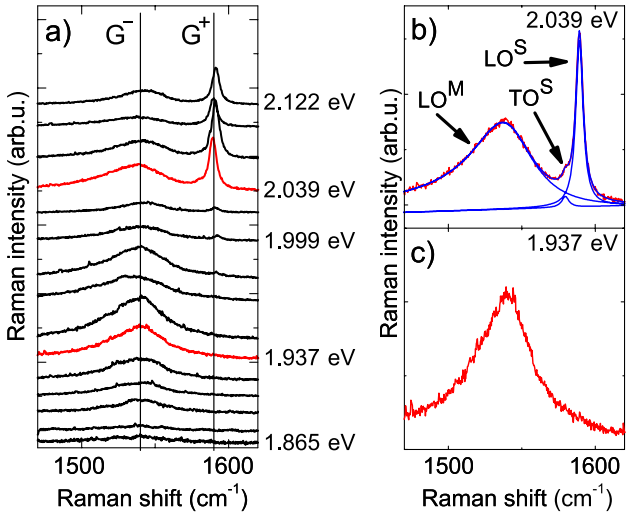

FIG. 2 (color online). (a) High-energy mode Raman spectra for excitation energies in the range of the Rayleigh-scattering maxima of Fig. 1 (1.87 to 2.12 eV). G^- and G^+ show different resonance conditions with a maximum Raman intensity at 1.95 eV excitation energy for G^-. (b) Spectrum obtained at 2.04 eV excitation energy; such a spectrum would typically be called a "metallic" Raman spectrum. Peaks are labeled by the associated phonon, LO or TO, where the superscript S indicates the semiconducting and M the metallic nanotube. (c) The excitation energy 1.94 eV meets only the resonance condition of the metallic nanotube; the G^+ peak is not observed.

In addition to the HEM spectra, we collected Raman spectra of the radial breathing mode at each excitation energy. We observed two RBM peaks at 217 cm^{-1} (RBM_1) and 140 cm^{-1} (RBM_2), corresponding to the two nanotubes. Both RBM features go through resonance (Fig. 3), with RBM_1 (RBM_2) having its maximum intensity at excitation energy similar to that of the G^- (G^+) mode. From the correlation of resonance energies we conclude that the G^- feature originates from the same tube as RBM_1 and G^+ from the same as RBM_2. In Fig. 3 we plot the intensities of both RBM peaks as a function of excitation energy. Fitting a Raman resonance profile to the data yields transition energies E_{ii} of 1.937 eV for RBM_1 and 2.04 eV for RBM_2 [26]. These energies match the energies of the two lower peaks in the Rayleigh spectrum in Fig. 1.

In order to assign the RBMs, and thus the high-energy G^- and G^+ peaks, to particular chiral indices (n_1, n_2) we identify the RBM frequency and its corresponding Raman resonance energy in an experimental and theoretical Kataura plot [2,3,27,28]. The Kataura plot in Fig. 4 shows theoretical data based on a nonorthogonal tight binding model from Ref. [29] and experimental values ($\times$ symbols) from Ref. [27]. Our results for RBM_1 and RBM_2 are marked by crosses in Fig. 4. The transition energies of nanotubes depend on the nanotube environment, whereas the RBM frequencies hardly change [3,30,31]. Assuming negligible deviation of the RBM frequency and a redshift (159 meV) of the transition energies in our sample compared to the data in Fig. 4, we assign RBM_1 to the metallic (12,3) tube. Although we cannot assign the second nanotube to a specific (n_1, n_2) chirality, its RBM frequency and resonance energy clearly show that it is semiconducting (see Fig. 4).

As a consequence of the (n_1, n_2) assignment, we can relate the high-energy modes G^- and G^+ to metallic and semiconducting tubes, respectively, independent of assumptions concerning the line shape of G^- and G^+. This result confirms previous experimental results and theoretical predictions about a strongly broadened and downshifted LO phonon in metallic nanotubes [9,12,13,15]. Furthermore, we show that the sharp peak at 1590 cm^{-1} (G^+) is related to a semiconducting nanotube. We can exclude the possibility that this peak originates from the TO phonon of the same metallic tube as the G^- mode because of the different resonance conditions for the G^- and G^+ features.

Furthermore the frequency of the G^+ peak is higher than expected for the TO phonon in metallic nanotubes. The frequency of the TO mode in metallic tubes is expected to be similar to that in semiconducting tubes [9,12]. Experimental results on isolated semiconducting nanotubes show that the TO phonon frequency for nanotubes with diameters similar to our tubes (1.1 and 1.8 nm) is $\approx$1570 cm^{-1}, thus lying well below 1590 cm^{-1} [32]. Only for nanotubes with large diameters ($d > 5$ nm) does the TO frequency approach 1590 cm^{-1}.

Therefore, a line shape like that of Fig. 2(b) with both a broad and downshifted metallic G^- and an additional G^+ peak located at 1590 cm^{-1} can best be explained by the presence of at least one metallic and one semiconducting tube. Even if only the metallic line shape as shown in Fig. 2(c) is observed and the experiment is limited to a small number of excitation wavelengths, we cannot exclude the possibility that the sample contains an additional semiconducting nanotube that does not benefit from resonant enhancement. It seems that often a "metallic" spec-

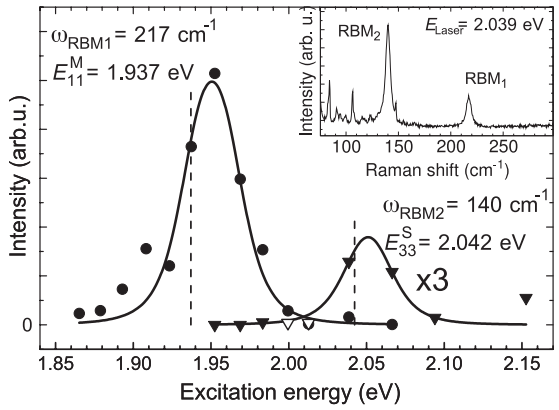

FIG. 3. Raman intensities of the radial breathing modes RBM_1 (circles) and RBM_2 (triangles) as a function of excitation energy. Open symbols are used when no nanotube signal was observed due to the overlapping signal from the atmosphere (sharp lines for small Raman shifts, see RBM spectrum in the inset). Fitting a Raman resonance profile to the data yields the transition energies E_{11}^{M-} for RBM_1 (metallic tube) and E_{33}^{S} for RBM_2 (semiconducting tube). The vertical dashed lines indicate the fitted optical transition energies.

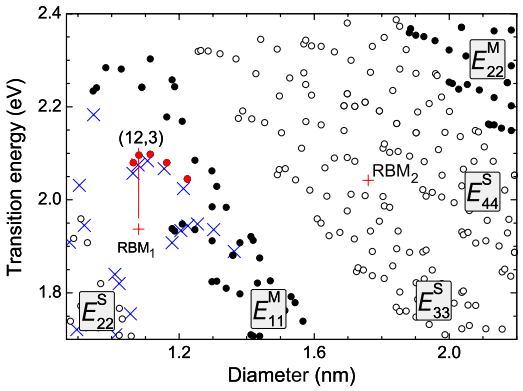

FIG. 4 (color online). Kataura plot containing theoretical data by Popov *et al.* [29] (open and closed circles) and experimental data ($\times$ symbols) from Ref. [27]. Theoretical data are upshifted by $\approx$ 300 meV according to Ref. [29]. Results from this work, RBM_1 and RBM_2, are given by crosses. Considering screening effects RBM_1 is assigned to the metallic (12,3) tube. RBM_2 cannot be assigned to a particular nanotube but certainly originates from a semiconducting tube excited resonantly into the third E_{33}^{S} or forth E_{44}^{S} optical transition.

trum like that in Fig. 2(b) arises from a small bundle instead of a single metallic nanotube [15,17,19,25]. In larger diameter metallic tubes, the G^- is less downshifted, and the spectrum will be more similar to that of semiconducting tubes [9,12].

After assigning the observed high-energy modes to LO vibrations, the question arises whether we can observe the TO phonons as well. In fact, the G^+ peak (LO of the semiconducting tube) shows a small shoulder [see Fig. 2 (b)], which we fit to a weak peak lying 9 cm^{-1} below the principal G^+ feature. For a semiconducting nanotube with a diameter of 1.8 nm, as in our experimental sample, theory and experiment predict the TO phonon frequency 10 to 20 cm^{-1} below the LO frequency [9,12,32]. Therefore we assign the shoulder of the G^+ peak to the TO phonon in the semiconducting nanotube. When only the metallic nanotube is in resonance [Fig. 2(c)] we cannot resolve a TO peak next to the G^- peak. The reason for the absence or very weak intensity of the TO peak might be that the (12,3) tube is close to a zigzag tube for which the TO phonon is Raman forbidden by symmetry [33].

Finally we want to make a remark on the defect induced Raman mode (D mode) which has not been investigated systematically in this work. We recorded the D mode spectrum at an excitation energy of 1.999 eV where both nanotubes are observed [Fig. 2(a)]. This spectrum showed no signal of the D mode, which agrees with our general experience on separated nanotubes in solution.

In conclusion, we presented Raman and Rayleigh-scattering experiments on a pair of one metallic and one semiconducting nanotube. With the assistance of the radial breathing Raman mode and Rayleigh-scattering spectra we assigned the high-energy Raman modes, a broad G^- peak at 1540 cm^{-1} and a sharp G^+ peak at 1590 cm^{-1} to the metallic and semiconducting nanotube, respectively. Considering theoretical predictions we show that both peaks, G^- and G^+, originate from the LO phonon, with G^- in metallic and G^+ in semiconducting tubes. We conclude that in a spectrum with a downshifted G^-—indicating a small diameter metallic nanotube—the presence of the G^+ peak at 1590 cm^{-1} indicates an additional semiconducting nanotube. Our experiments thus clearly favor the strong electron-phonon coupling of the LO mode in metallic nanotubes over the phonon-plasmon coupling model.

J. M. and C. T. acknowledge support from the Cluster of Excellence Unifying Concepts in Catalysis coordinated by the Technische Universität Berlin and funded by the Deutsche Forschungsgemeinschaft. J. M. acknowledges support also from the Alexander von Humboldt Foundation. The authors at Columbia University acknowledge support from the U.S. National Science Foundation (NIRT Grant No. ECS-05-07111).

*telg@physik.tu-berlin.de

[1] S. Reich, C. Thomsen, and J. Maultzsch, *Carbon Nanotubes: Basic Concepts and Physical Properties* (Wiley-VCH, Berlin, 2004).
[2] J. Maultzsch and C. Thomsen, in *AMN: Advanced Micro and Nanosystems*, edited by C. Hierold (Wiley-VCH, Weinheim, 2008), Vol. 8.
[3] J. Maultzsch, H. Telg, S. Reich, and C. Thomsen, Phys. Rev. B **72**, 205438 (2005).
[4] R. Krupke, F. Hennrich, H. v. Löhneysen, and M. M. Kappes, Science **301**, 344 (2003).
[5] M. S. Strano *et al.*, Science **301**, 1519 (2003).
[6] M. Zheng *et al.*, Science **302**, 1545 (2003).
[7] M. A. Pimenta *et al.*, Phys. Rev. B **58**, R16 016 (1998).
[8] A. Jorio *et al.*, Phys. Rev. B **66**, 115411 (2002).
[9] O. Dubay, G. Kresse, and H. Kuzmany, Phys. Rev. Lett. **88**, 235506 (2002).
[10] K. Kempa, Phys. Rev. B **66**, 195406 (2002).
[11] M. Lazzeri, S. Piscanec, F. Mauri, A. Ferrari, and J. Robertson, Phys. Rev. B **73**, 155426 (2006).
[12] S. Piscanec, M. Lazzeri, J. Robertson, A. C. Ferrari, and F. Mauri, Phys. Rev. B **75**, 035427 (2007).
[13] Y. Wu *et al.*, Phys. Rev. Lett. **99**, 027402 (2007).
[14] H. Telg, J. Maultzsch, S. Reich, and C. Thomsen, in *Electronic Properties of Novel Nanostructures*, edited by H. Kuzmany, J. Fink, M. Mehring, and S. Roth, AIP Conf. Proc. No. 786 (AIP, New York, 2005), p. 162.
[15] M. Oron-Carl, F. Hennrich, M. Kappes, H. Löhneysen, and R. Krupke, Nano Lett. **5**, 1761 (2005).
[16] J. Yan, Y. Zhang, P. Kim, and A. Pinczuk, Phys. Rev. Lett. **98**, 166802 (2007).
[17] J. Maultzsch, S. Reich, U. Schlecht, and C. Thomsen, Phys. Rev. Lett. **91**, 087402 (2003).
[18] C. Jiang *et al.*, Phys. Rev. B **66**, 161404(R) (2002).
[19] A. Jorio *et al.*, Phys. Rev. B **65**, 155412 (2002).
[20] A. Gaur and M. Shim, Phys. Rev. B **78**, 125422 (2008).
[21] L. Huang, X. Cui, B. White, and S. P. O'Brien, J. Phys. Chem. B **108**, 16451 (2004).
[22] K. Matsuda *et al.*, Appl. Phys. Lett. **86**, 123116 (2005).
[23] F. Simon, R. Pfeiffer, and H. Kuzmany, Phys. Rev. B **74**, 121411 (2006).
[24] M. Y. Sfeir *et al.*, Science **306**, 1540 (2004).
[25] M. Paillet, P. Poncharal, A. Zahab, and J.-L. Sauvajol, Phys. Rev. Lett. **94**, 237401 (2005).
[26] C. Thomsen and S. Reich, in *Light Scattering in Solids IX*, edited by M. Cardona and R. Merlin (Springer, Berlin, 2007), p. 120.
[27] H. Telg, J. Maultzsch, S. Reich, F. Hennrich, and C. Thomsen, Phys. Rev. Lett. **93**, 177401 (2004).
[28] R. Pfeiffer, F. Simon, H. Kuzmany, and V. N. Popov, Phys. Rev. B **72**, 161404 (2005).
[29] V. N. Popov, L. Henrard, and P. Lambin, Phys. Rev. B **72**, 035436 (2005).
[30] C. Fantini *et al.*, Phys. Rev. Lett. **93**, 147406 (2004).
[31] M. O'Connell, S. Sivaram, and S. Doorn, Phys. Rev. B **69**, 235415 (2004).
[32] M. Paillet *et al.*, Phys. Rev. Lett. **96**, 257401 (2006).
[33] M. Damnjanović, I. Milošević, T. Vuković, and R. Sredanović, Phys. Rev. B **60**, 2728 (1999).